Electronic Supplementary Material (ESI) for Nanoscale.
This journal is © The Royal Society of Chemistry 2019

# Supporting Information

# Functionalized Nanographene Sheets with High Antiviral Activity Through Synergistic Electrostatic and Hydrophobic Interactions

*Ievgen S. Donskyi, Walid Azab, Jose Luis Cuellar-Camacho, Guy Guday, Andreas Lippitz, Wolfgang E.S. Unger, Klaus Osterrieder, Mohsen Adeli,* and Rainer Haag**

## Table of contents

**Methods** ..... **1**
**Materials** ..... **5**
**Experimental Section** ..... **6**
**Characterization** ..... **8**
**Figure S1.** ..... **8**
**Table S1.** ..... **8**
**Figure S2.** ..... **9**
**Figure S3.** ..... **9**
**Table S2.** ..... **9**
**Table S3.** ..... **11**
**Figure S4** ..... **12**
**Figure S5.** ..... **12**
**Figure S6.** ..... **13**
**Figure S7.** ..... **13**
**Figure S8.** ..... **14**
**Figure S9.** ..... **14**
**References** ..... **14**

## Methods

*Zeta-potential measurements.* Zeta-potential experiments were performed on a Malvern zetasizer nano machine at 25 °C. Millipore water was used in all experiments. Measurements were performed with a Malvern-folded capillary zeta cell in automatic mode.

*Nano Tracking Analysis (NTA).* NTA measurements were performed on a Malvern NanoSight NS500 (Malvern, Malvern, UK) equipped with a SCMOS camera (Malvern, Malvern, UK) and a 635 nm laser under a scattering angle of 100° at 25 °C. Video capturing was

performed with a shutter length, shutter setting, and slider gain set at 2.5, 100, and 200, respectively. For each sample, 3 videos of 30-s at 25 FPS were recorded. Analysis was carried out using the NTA 3.0 0064 software (Malvern, Malvern, UK).

*Sample preparation for biological assays.* Solutions (5 mg/ml) of all nanographene derivatives in PBS were sonicated for 15 minutes, centrifuged at 8,000 rpm for 5 min at 4 °C, and the supernatant was collected. The concentration of nanoparticles in the supernatant was determined by nanotracking analysis (NTA) using a Malvern NanoSight NS500 device.[1] The concentration of the supernatants was converted from particles/mL to molar concentration using Avogadro's number ($6.02*10^{23}$ particles/mol).

*X-ray photoelectron spectroscopy (XPS) experiments*. Gold substrates for X-ray photoelectron spectroscopy (XPS) analysis were cleaned in a piranha solution (1:4) 30% $H_2O_2$ / 98% $H_2SO_4$ (v/v) during ultrasonication at room temperature for 10 min. Then they were washed with the DI water 5 times and with acetone 2 times. After drying overnight, the studied compounds were dissolved in methanol and evenly distributed dropwise across the surface of gold substrates. XPS spectra were recorded using a Kratos Axis Ultra DLD spectrometer equipped with a monochromatized Al Kα X-ray source (1486.69 eV) using an analyzer pass energy of 80 eV for survey spectra that were used for quantification. High-resolution, core-level O1s, C1s, and S2p spectra were recorded in FAT (fixed analyzer transmission) mode at a pass energy of 20 eV. The electron emission angle was 60° and the source-to-analyzer angle was 60°. The binding energy scale of the instrument was calibrated following a Kratos analytical procedure that used ISO 15472 binding energy data. Spectra were recorded by setting the instrument to the hybrid lens mode and the slot mode providing approximately a 300 x 700 $\mu m^2$ analysis area and using charge neutralization. All XPS spectra were processed with the UNIFIT program (version 2017). A Gaussian/Lorentzian product function peak shape model GL (30) was used in combination with a Shirley background. If not otherwise denoted, the L-G mixing for component peaks in all spectra were constrained to the value of 0.39. The S2p core level spectra were fitted with doublets of a constrained doublet separation of 1.2 eV, a peak area ratio of S2p 3/2:S2p 1/2 = 2:1, and equal FWHMs for S2p 3/2 and S2p 1/2. Peak fitting of C1s spectra was performed by using an asymmetric peak shape model for the graphene C1s component peak and a symmetric peak shape model for all other component peaks. After peak fitting of the C1s spectra, all the binding energies were calibrated in reference to the graphene C1s component at a binding energy of 284.6 eV.

*Near edge X-ray absorption fine structure (NEXAFS) experiments*: NEXAFS measurements were carried out at the synchrotron radiation source BESSY II (Berlin, Germany) at the HE-SGM monochromator dipole magnet CRG beamline. NEXAFS spectra were acquired

in total energy electron yield (TEY) mode using a channel plate detector. The resolution E/ΔE of the monochromator at the carbonyl π* resonance (hν = 287.4 eV) was in the order of 2500. Raw spectra were divided by ring current and monochromator transmission, the latter obtained with a freshly sputtered Au sample.[2] Alignment of the energy scale was achieved by using an $I_0$ feature referenced to a C1s → π* resonance at 285.4 eV measured with a fresh surface of HOPG (highly ordered pyrolytic graphite, Advanced Ceramic Corp., Cleveland, USA).[3] If not otherwise denoted, all NEXAFS spectra are shown after subtraction of the pre-edges followed by normalization of the post-edge count rates to one.[2] All C K-edges were measured at 55° incident angle of the linearly polarized synchrotron light beam.

*Scanning Force Microscopy (SFM)*. Samples were prepared by spin casting dispersions of graphene materials (0.1 mg/mL) in deionized water onto freshly cleaved mica substrates at 50 rps for 60 seconds. The mica substrates were mounted onto Ø12 mm stainless steel discs with double-sided tape. Measurements were performed using a Bruker Multimode 8, Nanoscope 5 with a J-type scanner, operated in tapping mode with Nanosensors PPP-NCLR cantilever tips with a typical resonant frequency of 190 kHz, a spring constant of 48 N $m^{-1}$, and a tip radius of < 10 nm. Images were recorded at a minimum resolution of 1024 x 1024 and a scan speed of 0.8 Hz or lower. All experiments were conducted under ambient conditions, and results were analyzed using the Bruker NanoScope Analysis 1.8 software, along with Gwyddion. Images were line-flattened using a first order (linear) fit.

*Virus and Cells.* HSV-1 bacterial artificial chromosome (pYEbac102) was kindly provided by Dr. Yasushi Kawaguchi, Institute of Medical Science, The University of Tokyo.[4] The virus was reconstituted on Vero cells using Lipofectamine 2000 (Invitrogen). The enhanced green fluorescent protein (EGFP) gene was integrated into the virus genome to facilitate detection of virus replication in infected cells. African green monkey kidney (Vero) cells were grown in DMEM medium (PAN Biotech) supplemented with 10% fetal calf serum (FCS, PAN Biotech), 100 U/mL penicillin (Roth), and 100 µg/mL streptomycin (Alfa Aesar).

*Cell viability assay.* Vero cells were incubated with different nanographene derivatives for 24 h, and cell viability was determined using the WST-1 assay (Cayman Chemicals).[5] Briefly, cells were grown in 96-well plates and incubated with nanographene derivatives (1.6 fM) for 1 h at 4 °C. The plates were moved to the incubator at 37 °C and further incubated for 24 h. The WST-1 mixture was added to the cells and, after 2 h incubation at 37 °C, absorbance of each sample was read using a microplate reader (Berthold Technologies) at 450 nm wavelength. Mock cells (untreated with nG derivatives) and cells treated with 0.1% $H_2O_2$ (Sigma) for 30 s were used as controls.

*Flow cytometry.* To determine the $EC_{50}$, HSV-1 at MOI of 1 was mixed with nanographene derivatives (at concentrations ranged from $10^3$ to $10^6$) for 30 min at room temperature. The mixture was added to a confluent monolayer of Vero cells and incubated at 37 °C. After 24 h, cells were trypsinized, washed twice with cold PBS, and centrifuged at 8000 rpm for 5 min. The supernatant was discarded, cells were resuspended in PBS, and EGFP expression in 10,000 cells was quantified with a CytoFLEX flow cytometer (Beckman Coulter) to determine the percentage of infection. Infection induced by HSV-1 without previous treatment with nanographene derivatives was set to 100%.

*Plaque reduction assay.* Vero cells were grown in 24-well plates. HSV-1 [100 PFU per well] were incubated with nanographene derivatives (1.6 fM) for 30 min at room temperature, and the mixture was added to the cells. After 1 h incubation at 37 °C, cells were washed with PBS and the remaining un-entered viruses were inactivated with citrate buffer pH 3 [40 mM citric acid, 135 mM NaCl, and 10 mM KCl] for 30 s. The cells were washed again with PBS and overlaid with DMEM containing 0.5% methylcellulose.[6] After 48 h, green-fluorescent plaques were counted under an inverted fluorescence microscope (Zeiss Axiovert 100) and the mean of three independent experiments was calculated. The cells were then fixed with 4% paraformaldehyde and the plaques were stained with 0.75% crystal violet. Mock-infected cells and HSV-1-infected cells without nanographene derivatives were used as controls. Plaque numbers induced by parental HSV-1 without previous treatment with nanographene derivatives were set to 100%.

*Statistical analysis.* All viability, flow cytometry-based, and plaque reduction assays were repeated three independent times. Statistical evaluation was performed using GraphPad Prism 5 (GraphPad software). One-way and two-way ANOVA was used to test for significance. Bonferroni adjustment was applied for multiple comparisons. Data represent mean values, and standard deviations are indicated by error bars. P values less than 0.05 are considered significant.

*Atomic force microscopy within a fluid chamber.* Imaging of the interaction of nanographene derivatives with HSV to account binding was performed in PeakForce mode with a maximal loading force of 500 pN. A Multimode 8 Nanoscope from Bruker with a nanocontroller V was used in all experiments with an assembled fluid chamber. All measurements were carried out in PBS and at room temperature. Sample preparation is described as follows. Round discs of cleaved mica of about 1 cm in diameter were used as substrate. The mica discs were glued with a double-sided tape onto circular metal pucks to be then mounted on the AFM head. 5 µL of HSV-1 solution were deposited at the center of the mica and allowed to rest for 5 minutes. The negatively charged surface of mica was allowed to directly bind and image HSV particles. Imaging of nanographene sheets and the mixture of these sheets with HSV

was achieved after coating the mica surface with the cationic polymer poly-L-lysine. 10 μL of poly-L-Lysine solution (Sigma-Aldrich MW: 75,000-120,000) was deposited at the center of cleaved mica and allowed to dry. Afterwards the mica surface was rinsed with water repeatedly and allowed to dry again. Then 5 μL of only nanographene sheets solution or the mixture of the sheets with HSV were deposited and incubated for 10 minutes. Subsequently the sample was slightly blotted with filter paper without allowing it to dry, but only to reduce the amount of sample on the surface to a thin film. The sample was then immediately mounted on the AFM head and a closed fluid chamber was assembled. All measurements were performed in PBS. SNL tips with a nominal tip radius of 2 nm and spring constant of 0.35 N/m were used and cantilevers were calibrated on clean mica substrates before all experiments. Images were taken with a 512 point per line and 0.7 Hz scan rate.

*Nuclear Magnetic Resonance (NMR).* NMR spectra were performed on a Brucker AMX 500, Brucker Avance 400 spectrometer or Jeol ECP 500. For internal calibration tetramethylsilane was used at 12 MHz with complete proton decoupling.

*Gel Permeation Chromatography (GPC).* GPC measurements were performed using Agilent 1100 solvent delivery system with a manual injector, an isopump, and an Agilent 1100 differential refractometer. A Brookhaven BI-MwA7-angle light scattering detector was coupled to the size exclusion chromatography (SEC) to determine the molecular weight for each fraction of the polymer that were eluted from the SEC columns. For separating the polymer samples, three 30 cm columns were used (10μm PSS Suprema columns with pore sizes of 100 Å, 1000 Å, and 3000 Å). Water was used as the mobile phase; the flow rate was set at 1.0 mL/min. All columns were kept at room temperature (RT). For each measurement, 100 μL of sample was injected with a concentration of 5 mg/mL solution. For acquisition of the data from seven scattering angles (detectors) and differential refractometer a WinGPC Unity from PSS was used. Molecular weight distributions and molecular weights were determined by comparison with Pullulan standards (10 different sizes from 342 to 710,000 g/mol). Water was used as a solvent containing 0.1 M $NaNO_3$.

**Materials**

Graphite powder (median diameter 7-10 microns) was purchased from ACROS Organics. Glycidol (SigmaAldrich) was dried over $CaH_2$, distilled before use, and stored at 4 °C. Polyglycerol (PG) ($M_n$ = 3,700 $g^*mol^{-1}$) was prepared according to a published procedure. Sodium hypochlorite (11-14% available chlorine), potassium tert-butoxide in THF (1 M), methanesulfonyl chloride (MsCl) (≥ 99.7%), triphenylphoshine ($PPh_3$) (99%), sulfur trioxide

pyridine complex ($Py^{\bullet}SO_3^-$) (98%), phosphate buffer solution 1.0 M, pH 7.4 (25 °C) N,N-dimethylformamide (DMF) (≥ 99.8%), 1-methyl-2-pyrrolidinone (NMP) (99.5%), 1-propylamine ($C_3H_7$-$NH_2$) (98%), 1-hexylamine ($C_6H_{13}$-$NH_2$) (99%), 1-nonylamine ($C_9H_{19}$-$NH_2$) (99.5%), 1-dodecylamine ($C_{12}H_{25}$-$NH_2$) (98%), 1-octadecylamine ($C_{18}H_{37}$-$NH_2$) (97%) were purchased from Sigma Aldrich. 2,4,6-trichloro-1,3,5-triazine (TCT) (99%) and sodium azide ($NaN_3$) (99%) were purchased from Acros Organics. Sodium hydroxide (NaOH) (99%) was purchased from Fisher Chemical. Anhydrous solvents were either obtained from solvent purification (MBraun MB-SPS-800) system or purchased as ultra-dry solvents from Acros Organics. Water was derived from a Milli-Q advantage A10 water purification system in all experiments. Biotech cellulose ester dialysis bags MWCO 20 kDa were purchased from Spectrum labs. All chemical compounds were used without further purification.

**Experimental Section**

*Production of nanographene (nG).* Graphite powder (10 g) was dispersed in a solution of 100 ml of sodium hypochlorite solution (15%) and 100 ml of deionized water. The dispersion was heated to 40 °C and stirred for 7 days. Then the mixture was purified by repeated centrifugation (3 times, 8,000 rpm, 30 minutes) and washing with deionized water until the neutral pH of the supernatant. Further sonication was performed using a Bandolin Sonorex RK510H for 60 min to exfoliate the nanographene with a nominal power of 160 W. The solution was left overnight, then the supernatant was collected and centrifuged at 2000 rpm to remove the remaining multi-layer sheets or suspended graphite particles. The product was then lyophilized. Yield 20%.

*Synthesis of nG-Trz*. *S*ynthesis of nG-Trz were conducted according to our recently reported method (yield 78%).[7]

*Synthesis of Polyglycerol (PG)*. PG was synthesized according to a reported procedure (yield 81%).[8] $M_n$ = 3.7 kDa.

*Synthesis of polyglycerol with a few amino groups (PG-$NH_2$ 5%)*. Polyglycerol with 5% amino functional groups was synthesized according to the procedure reported in the literature.[9] The hyperbranched polyglycerol (PG, $M_n$ = 3.8 kDa) was initially mesylated and subsequently azidated to convert the hydroxyl to azide functional groups with further reduction to the amino functional groups forming amino-functionalized PG (yield 60%). *Polyglycerol-mesylate*. $^1$H NMR (500 MHz, $D_2O$, δ): 4.2 – 3.4 (PG backbone), 3.3 – 3.2 ($CH_3$). *Polyglycerol-azide*. $^1$H NMR (500 MHz, $D_2O$ δ): 4.1 – 3.4 (PG backbone). *PG-amine with 5% amino-functional groups*. $^1$H NMR (500 MHz, $D_2O$ δ): 4.0 – 3.3 (PG backbone).

*Synthesis of graphene sheets with polyglycerol coverage (nG-PG)*. nG-Trz (0.3 g) was dispersed in NMP (50 mL) and sonicated for 2 hours followed by stirring in an ice bath. *PG-$NH_{2(5\%)}$* (0.96 g, 0.08 mmol) was dissolved in NMP (50 mL) and added into nG-Trz mixture at 0 °C followed by stirring at 0 °C for 2 hours. Triethylamine ($Et_3N$) (0.17 mL, 1.25 mmol) was added into the mixture and stirred for 1 hour at 0 °C. The temperature of the mixture was increased to 25 °C and it was stirred for 3 days. Then the mixture was dialyzed by a dialysis bag (cutoff MWCO 20 kDa) against water for 5 days and freeze-dried (yield 80%).

*Sulfation of nG-PG (nG-PGS)*. nG-PG was sulfated according to the reported procedures in the literature.[10-12] Briefly, nG-PG (0.3 g) was dried by lyophilization and then suspended in dry DMF (20 ml). Afterwards, pyridine sulfur trioxide (1.25 g, 7.85 mmol) dissolved in 10 ml dry DMF was added to the above mixture and it was stirred at 60 °C for 24 hours. Then, DMF was decanted and deionized water (20 ml) was added to the reaction. Subsequently, the pH of the reaction mixture was adjusted to pH 8 using NaOH (10% w/v), and the solution was dialyzed by a dialysis bag (cutoff MWCO 20 kDa) against 1 M NaCl solution for 5 days and further against water for 7 days and then freeze-dried (yield 80%).

*Conjugation of primary amines with different lengths of aliphatic chains ($C_3H_7$-$NH_2$, $C_6H_{13}$-$NH_2$, $C_9H_{19}$-$NH_2$, $C_{12}H_{25}$-$NH_2$, $C_{18}H_{37}$-$NH_2$) to nG-PGS.* nG-PGS (0.1 g) was dispersed in DMF (25 mL) and sonicated at room temperature for 30 minutes. Fatty amines with different alkyl chains ($C_3H_7$-$NH_2$, $C_6H_{13}$-$NH_2$, $C_9H_{19}$-$NH_2$, $C_{12}H_{25}$-$NH_2$, $C_{18}H_{37}$-$NH_2$) (42 μmol) were dissolved in DMF (15 mL) and added to the nG-PGS dispersion at 25 °C. The mixture was stirred at this temperature for 2 hours and then $Et_3N$ (5.6 μL, 0.042 mmol) was added to the reaction flask and stirred at 60 °C for 48 hours. The product was dialyzed (MWCO 20 kDa) against water/isopropanol 1/1 mixture for 7 days. The solvent was evaporated, and the product was dried by lyophilization (yield 80-85%).

## Characterization

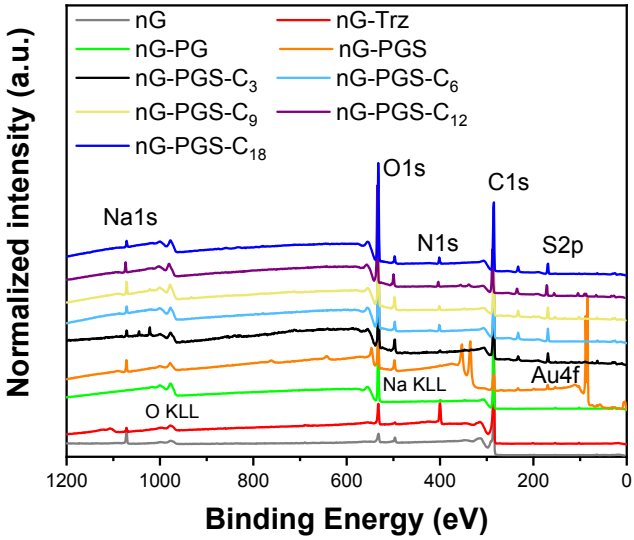


**Figure S1.** (a) Survey XPS spectra of the nG, nG-trz, nG-PG, nG-PGS, nG-PGS-$C_3$, nG-PGS-$C_6$, nG-PGS-$C_9$, nG-PGS-$C_{12}$, nG-PGS-$C_{18}$. For assignments and element ratios see Table S1.

**Table S1.** Relative element fractions and C/O atomic ratio obtained by quantification of the XPS spectra displayed in Figure S1a.

| Sample | C/O ratio | C at% | N at% | S at% |
|---|---|---|---|---|
| nG | 23.5 | 94.0 | - | - |
| nG-Trz | 12.9 | 81.4 | 11.0 | - |
| nG-PG | 2.3 | 68.0 | 0.9 | - |
| nG-PGS | 1.5 | 54.5 | 0.9 | 4.8 |
| nG-PGS-$C_3$ | 2.3 | 61.9 | 1.1 | 2.8 |
| nG-PGS-$C_6$ | 2.3 | 63.7 | 3.1 | 4.6 |
| nG-PGS-$C_9$ | 1.6 | 54.6 | 2.1 | 5.0 |
| nG-PGS-$C_{12}$ | 1.7 | 55.4 | 2.7 | 5.3 |
| nG-PGS-$C_{18}$ | 2.4 | 64.2 | 3.0 | 3.8 |

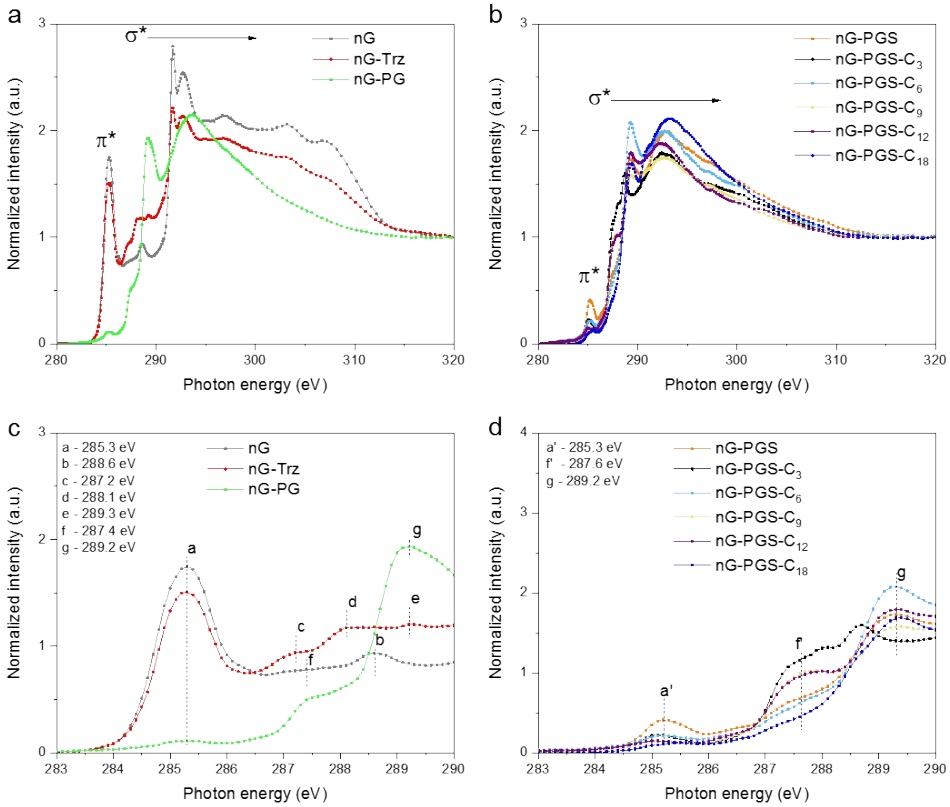


**Figure S2.** (a), (b) C K-edge and (c), (d) expanded C K-edge NEXAFS of of nG, nG-trz, nG-PG, nG-PGS, nG-PGS-$C_3$, nG-PGS-$C_6$, nG-PGS-$C_9$, nG-PGS-$C_{12}$, nG-PGS-$C_{18}$. For assignments see Table S3.

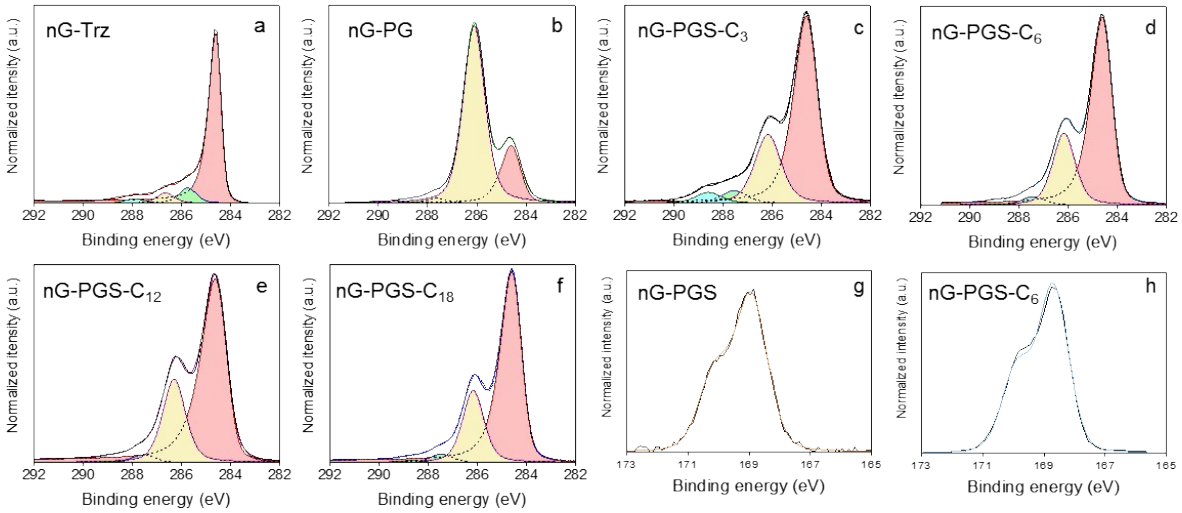


**Figure S3.** Highly resolved C1s XPS spectra with peak fitting for (a) nG-Trz, (b) nG-PG, (c) nG-PGS-$C_3$, (d) nG-PGS-$C_6$, (e) nG-PGS-$C_{12}$, (f) nG-PGS-$C_{18}$, highly resolved S2p spectra of (g) nG-PGS, and (h) nG-PGS-$C_6$ are similar to all S2p spectra of sulfated nanomaterials. For assignments and full spectra see Table S2.

**Table S2.** Spectroscopic parameters of XPS spectra of nG-trz, nG-PG, nG-PGS, nG-PGS-$C_3$, nG-PGS-$C_6$, nG-PGS-$C_9$, nG-PGS-$C_{12}$, nG-PGS-$C_{18}$, obtained by peak fitting using the UNIFIT software.

| Sample | Spectrum | Binding energy | L-G Mixing | FWHM | Interpretation | Relat. Area | Abs. Area |
|---|---|---|---|---|---|---|---|

| | | | | | | | |
|---|---|---|---|---|---|---|---|
| nG | C 1s | 284.6 | 0.39 | 0.6 | C–C $sp^2$ | 0.96 | 33443 |
| | | 286.4 | 0.39 | 0.9 | C–O–C, C–O–H | 0.02 | 776 |
| | | 291.5 | 0.39 | 0.8 | π–π* shake ups | 0.02 | 441 |
| nG-Trz | C1s | 284.6 | 0.39 | 0.6 | C–C $sp^2$ | 0.82 | 26917 |
| | | 285.7 | 0.39 | 0.8 | C–N=C | 0.09 | 2879 |
| | | 286.6 | 0.39 | 0.8 | C–Cl | 0.06 | 1979 |
| | | 287.9 | 0.39 | 0.8 | NH–C=O | 0.03 | 884 |
| nG-PG | C1s | 284.6 | 0.39 | 1.0 | C–C $sp^2$ | 0.23 | 8049 |
| | | 286.1 | 0.39 | 1.0 | C–O–C, C–O–H | 0.74 | 26391 |
| | | 287.6 | 0.39 | 1.0 | C=O | 0.02 | 745 |
| | | 288.7 | 0.39 | 1.0 | O–C=O | 0.01 | 172 |
| nG-PGS | C1s | 284.6 | 0.39 | 1.3 | C–C $sp^2$, C–C aliphatic | 0.61 | 10484 |
| | | 286.2 | 0.39 | 1.3 | C–O–C, C–O–S | 0.34 | 5880 |
| | | 287.6 | 0.39 | 1.3 | C=O | 0.04 | 638 |
| | | 288.6 | 0.39 | 1.3 | O–C=O | 0.01 | 208 |
| | S2p | 168.9 | 0.21 | 1.2 | S=O | 1 | 3446 |
| nG-PGS-$C_3$ | C1s | 284.6 | 0.39 | 1.1 | C–C $sp^2$, C–C aliphatic | 0.66 | 7561 |
| | | 286.2 | 0.39 | 1.2 | C–O–C, C–O–S | 0.26 | 2964 |
| | | 287.6 | 0.39 | 1.2 | C=O | 0.05 | 542 |
| | | 288.6 | 0.39 | 1.2 | O–C=O | 0.04 | 469 |
| | S2p | 168.6 | 0.26 | 1.2 | S=O | 1 | 1190 |
| nG-PGS-$C_6$ | C1s | 284.6 | 0.39 | 1.0 | C–C $sp^2$, C–C aliphatic | 0.70 | 18364 |
| | | 286.2 | 0.39 | 1.1 | C–O–C, C–O–S | 0.27 | 7041 |
| | | 287.4 | 0.39 | 1.1 | C=O | 0.03 | 836 |
| | | 288.8 | 0.39 | 1.1 | O–C=O | 0.01 | 122 |
| | S2p | 168.7 | 0.18 | 1.1 | S=O | 1 | 4574 |
| nG-PGS-$C_9$ | C1s | 284.6 | 0.39 | 1.1 | C–C $sp^2$, C–C aliphatic | 0.71 | 6376 |
| | | 286.2 | 0.39 | 1.1 | C–O–C, C–O–S | 0.27 | 2411 |
| | | 287.6 | 0.39 | 1.1 | C=O | 0.02 | 219 |
| | | 288.6 | 0.39 | 1.1 | O–C=O | 0.01 | 26 |
| | S2p | 168.7 | 0.17 | 1.1 | S=O | 1 | 3532 |
| nG-PGS-$C_{12}$ | C1s | 284.6 | 0.39 | 1.2 | C–C $sp^2$, C–C aliphatic | 0.70 | 16163 |
| | | 286.3 | 0.39 | 1.1 | C–O–C, C–O–S | 0.26 | 6098 |
| | | 287.6 | 0.39 | 1.1 | C=O | 0.03 | 561 |
| | | 288.8 | 0.39 | 1.1 | O–C=O | 0.01 | 87 |
| | S2p | 168.6 | 0.21 | 1.2 | S=O | 1 | 4514 |
| nG-PGS-$C_{18}$ | C1s | 284.6 | 0.39 | 1.0 | C–C $sp^2$, C–C aliphatic | 0.71 | 22108 |
| | | 286.2 | 0.39 | 1.0 | C–O–C, C–O–S | 0.25 | 7778 |
| | | 287.5 | 0.39 | 1.0 | C=O | 0.03 | 917 |
| | | 288.7 | 0.39 | 1.0 | O–C=O | 0.01 | 218 |
| | S2p | 168.7 | 0.20 | 1.1 | S=O | 1 | 4323 |

**Table S3.** Resonances in the C K-edge NEXAFS measured of nG-trz, nG-PG, nG-PGS, nG-PGS-$C_3$, nG-PGS-$C_6$, nG-PGS-$C_9$, nG-PGS-$C_{12}$, nG-PGS-$C_{18}$.

| Sample | | Photon energy | Assignment |
|---|---|---|---|
| nG | a | 285.3[3,13] | C1s → π* (C=C) |
| | b | 288.6[14] | C1s → σ* (C–O) |
| nG-Trz | a | 285.3[3,13] | C1s → π* (C=C) |
| | c | 287.2[7,15] | C1s → σ* (C–N) |
| | d | 288.1[7,15] | C1s → σ* (C–N) |
| | e | 289.3[7,15] | C1s → σ* (C–N) |
| nG-PG | a | 285.3[3,13] | C1s → π* |
| | f | 287.4[16] | C1s → σ* (C–O) |
| | g | 289.2[17] | C–H* |
| nG-PGS | a‘ | 285.3[3,13] | C1s → π* |
| | f‘ | 287.6[16] | C1s → σ* (C–O) |
| | g | 289.2[17] | C–H* |
| nG-PGS-$C_3$ | a‘ | 285.3[3,13] | C1s → π* |
| | f‘ | 287.6[16] | C1s → σ* (C–O) |
| | g | 289.2[17] | C–H* |
| nG-PGS-$C_6$ | a‘ | 285.3[3,13] | C1s → π* |
| | f‘ | 287.6[16] | C1s → σ* (C–O) |
| | g | 289.2[17] | C–H* |
| nG-PGS-$C_9$ | a‘ | 285.3[3,13] | C1s → π* |
| | f‘ | 287.6[16] | C1s → σ* (C–O) |
| | g | 289.2[17] | C–H* |
| nG-PGS-$C_{12}$ | a‘ | 285.3[3,13] | C1s → π* |
| | f‘ | 287.6[16] | C1s → σ* (C–O) |
| | g | 289.2[17] | C–H* |
| nG-PGS-$C_{18}$ | a‘ | 285.3[3,13] | C1s → π* |
| | f‘ | 287.6[16] | C1s → σ* (C–O) |
| | g | 289.2[17] | C–H* |

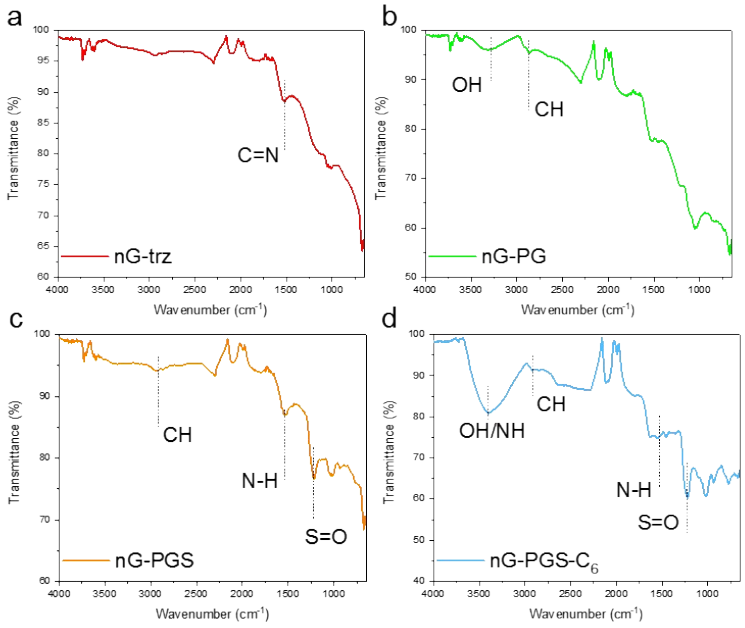


**Figure S4.** FTIR spectra of (a) nG-trz, (b) nG-PG, (c) nG-PGS, and (d) nG-PGS-$C_6$. Characteristic bands are denoted on the graphs. A broad absorbance band for C=N bonds of nG-Trz triazine moieties is observed at 1513 $cm^{-1}$ (a). Absorbance bands at 3303 and 2860 $cm^{-1}$ are assigned to characteristic O–H and C–H bonds of the polyglycerol molecules, respectively (b). Absorbance band at 1224 $cm^{-1}$ is assigned to S=O bonds of sulfate groups in nG-PGS and its derivatives (c,d). Similar spectra are obtained for all sulfated nG-PGS derivatives.

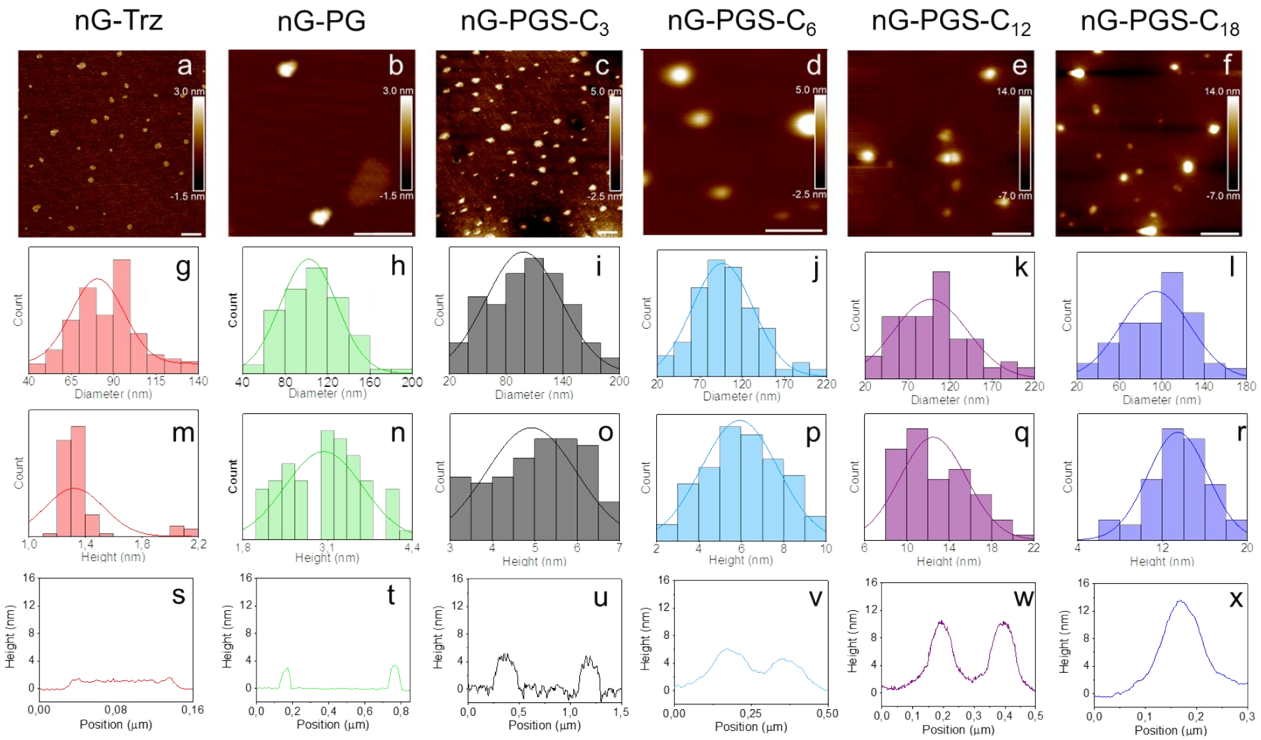


**Figure S5.** (a-f) AFM images with corresponding (g-l) diameter, (m-r) height histograms, and (s-x) height images for nG-Trz, nG-PG, nG-PGS-$C_3$, nG-PGS-$C_6$, nG-PGS-$C_{12}$, and nG-PGS-$C_{18}$, respectively. Scale bars correspond to 250 nm.

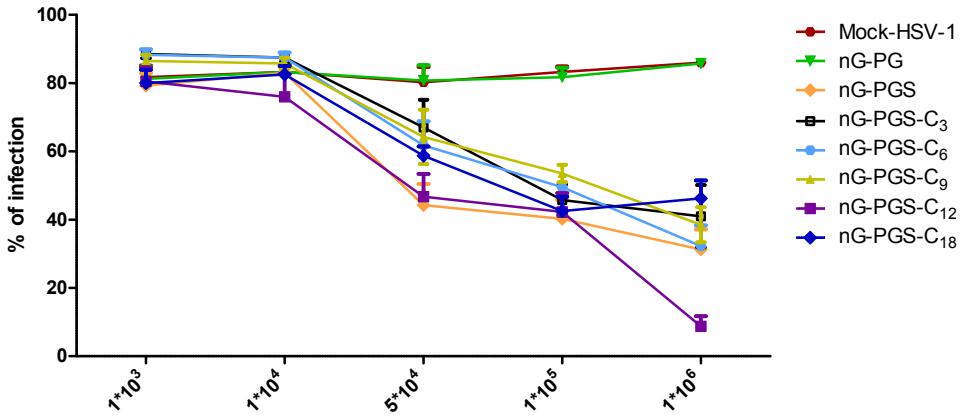


**Figure S6.** Infection of Herpes virus determined by flow cytometry for a range of concentrations of Moch-HSV-1, nG-PG, nG-PGS, nG-PGS-$C_3$, nG-PGS-$C_6$, nG-PGS-$C_9$, nG-PGS-$C_{12}$, and nG-PGS-$C_{18}$. The highest concentration of $1*10^6$ particles/ml corresponds to concentration 1.6 fM.

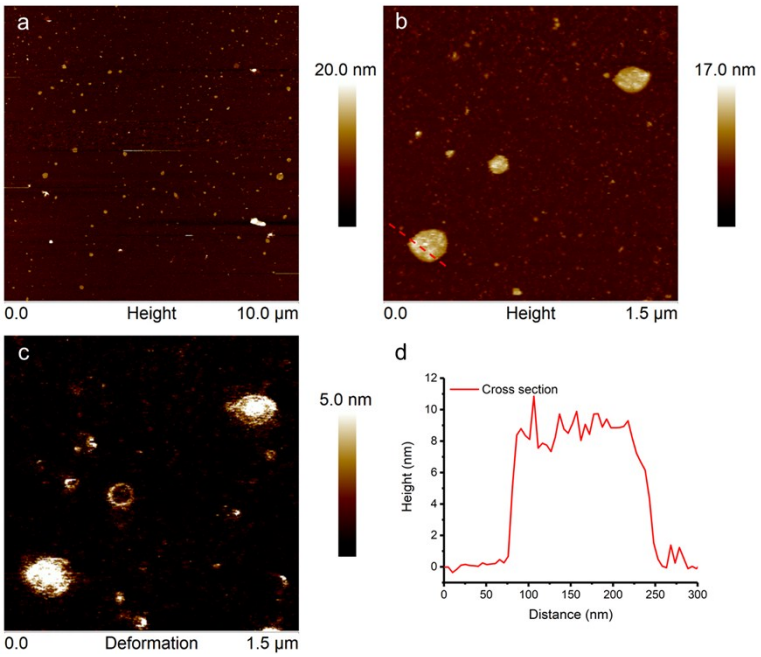


**Figure S7.** nG-PGS-$C_6$ sheets imaged by atomic force microscopy in PeakForce mode in PBS. (a), (b) show topographical images at two different scales where majority of sheets are observed to have a round-like shape. (c) shows a deformation map of (b) which accounts for the degree of AFM tip deformation into the surface. As can be observed in the color-coded scale and from the image, most deformation occurred where the sheets were located, which indicated that the AFM tip penetrated into the soft polymer cushion provided during functionalization. In (d) a cross-section profile of one of the sheets shown in (b) is presented, where a clear, almost constant plateau along the sheets' surface of about 8 nm was obtained.

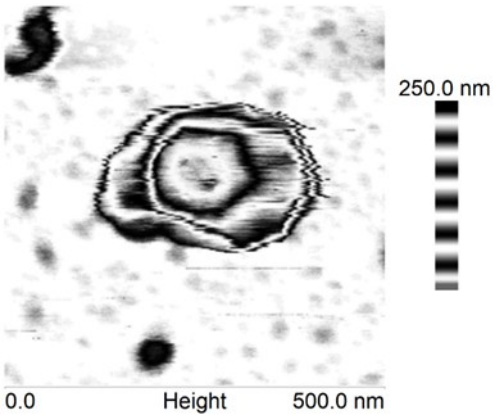


**Figure S8.** AFM imaging in PeakForce mode of single HSV particles. 2D image of surface of HSV shown in a different color-coded scale for a better visibility of the icosahedral viral capsid and the surrounding membrane.

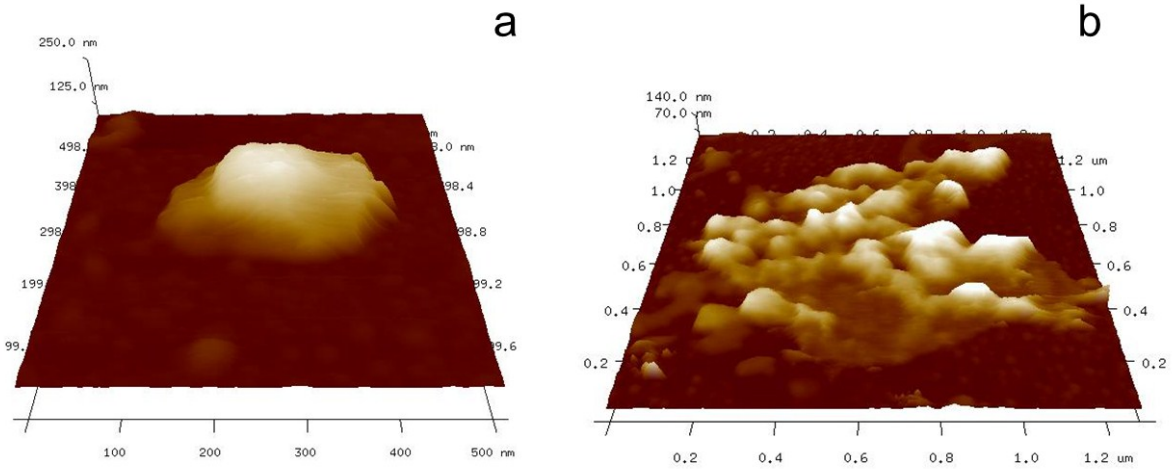


**Figure S9.** 3D reconstruction of (a) single HSV particle and (b) mixture of HSV with nG-PGS-$C_6$.

## References


1 M. Asadian-Birjand, C. Biglione, J. Bergueiro, A. Cappelletti, C. Rahane, G. Chate, J. Khandare, B. Klemke, M. C. Strumia, M. Calderón, *Macromol. Rapid Commun*., 2016, **37**, 439−445.
2 J. Stöhr, *NEXAFS Spectroscopy*, 1992, Springer, Berlin Heidelberg, 114-161.
3 P. E. Batson, *Phys. Rev. B*, 1993, **48**, 2608.
4 M. Tanaka, H. Kagawa, Y. Yamanashi, T. Sata, Y. Kawaguchi, *Journal of Virology*, 2003, **77**, 1382–1391.
5 K. Segawa, J. Suzuki, and S. Nagata, *Proc. Nat. Aca. Sci. USA*, 2011, **108**, 19246-19251.
6 P. Dey, T. Bergmann, J. L. Cuellar Camacho, S. Ehrmann, M. S. Chowdhury, M. Zhang, I. Dahmani, R. Haag, and W. Azab, *ACS Nano*, 2018, **12**, 6429-6442.
7 G. Guday, I. S. Donskyi, M. F. Gholami, G. Algara-Siller, F. Witte, A. Lippitz, W. E. S. Unger, B. Paulus, J. P. Rabe, M. Adeli, and R. Haag, *Small*, 2019, **15**, 1805430.
8 H. Frey, R. Haag, *Reviews in Molecular Biotechnology*, 2002, **90**, 257-267.
9 S. Roller, H. Zhou, R. Haag, *Molecular Diversity*, 2005, **9**, 305–316.
10 M. Weinhart, D. Gröger, S. Enders, J. Dernedde, R. Haag, *Biomacromolecules*, 2011, **12**, 2502–2511.
11 J. Dernedde, A. Rausch, M. Weinhart, S. Enders, R. Tauber, K. Licha, M. Schirner, U. Zügel, A. von Bonin, R. Haag, *Proc. Nat. Aca. Sci. USA*, 2010, **107**, 19679-19684.
12 I. Donskyi, M. Drüke, K. Silberreis, D. Lauster, K. Ludwig, C. Kühne, W. Unger, C. Böttcher, A. Herrmann, J. Dernedde, M. Adeli, and R. Haag, *Small*, 2018, **14**, e1800189.
13 C. Ehlert, W. E. S. Unger, P. Saalfrank, *Physical chemistry chemical physics PCCP,* **2014**, *16*, 14083.
14 C. Ehlert, Doctoral Thesis U Potsdam, 2016, https://publishup.uni-potsdam.de/frontdoor/index/index/docId/10484.
15 A. Faghani, I. S. Donskyi, M. F. Gholami, B. Ziem, A. Lippitz, W. E. S. Unger, C. Böttcher, J. P. Rabe, R. Haag, and M. Adeli, *Angew. Chem. Int. Ed*., 2017, **56**, 2675–2679.
16 K. H. Tan, S. Sattari, I. S. Donskyi, J. L. Cuellar-Camacho, C. Cheng, K. Schwibbert, A. Lippitz, W. E. S. Unger, A. Gorbushina, M. Adeli, and R. Haag, *Nanoscale*, 2018, **10**, 9525-9537.
17 H.Peisert, T.Chassé, P.Streubel, A.Meisel, and R.Szargan, *JESRP*, 1994, **68**, 321-328.